available at www.sciencedirect.com

**ScienceDirect**

www.elsevier.com/locate/molonc

# Enhanced anticancer activity of a combination of docetaxel and Aneustat (OMN54) in a patient-derived, advanced prostate cancer tissue xenograft model

*Sifeng Qu[a,b], Kendric Wang[b], Hui Xue[a], Yuwei Wang[a], Rebecca Wu[a], Chengfei Liu[c], Allen C. Gao[c], Peter W. Gout[a], Colin C. Collins[b,d], Yuzhuo Wang[a,b,d],\**

[a]Department of Experimental Therapeutics, BC Cancer Agency, Vancouver, BC, Canada
[b]Vancouver Prostate Centre, Vancouver, BC, Canada
[c]Department of Urology, University of California at Davis, Sacramento, CA, USA
[d]Department of Urologic Sciences, Faculty of Medicine, University of British Columbia, Vancouver, BC, Canada

## ARTICLE INFO

## ABSTRACT

The current first-line treatment for advanced metastatic prostate cancer, i.e. docetaxel-based therapy, is only marginally effective. The aim of the present study was to determine whether such therapy can be improved by combining docetaxel with Aneustat (OMN54), a multivalent botanical drug candidate shown to have anti-prostate cancer activity in preliminary *in vitro* experiments, which is currently undergoing a Phase-I Clinical Trial. Human metastatic, androgen-independent C4-2 prostate cancer cells and NOD-SCID mice bearing PTEN-deficient, metastatic and PSA-secreting, patient-derived subrenal capsule LTL-313H prostate cancer tissue xenografts were treated with docetaxel and Aneustat, alone and in combination. *In vitro*, Aneustat markedly inhibited C4-2 cell replication in a dose-dependent manner. When Aneustat was combined with docetaxel, the growth inhibitions of the drugs were essentially additive. *In vivo*, however, the combination of docetaxel and Aneustat enhanced anti-tumor activity synergistically and very markedly, without inducing major host toxicity. Complete growth inhibition and shrinkage of the xenografts could be obtained with the combined drugs as distinct from the drugs on their own. Analysis of the gene expression of the xenografts using microarray indicated that docetaxel + Aneustat led to expanded anticancer activity, in particular to targeting of cancer hallmarks that were not affected by the single drugs. Our findings, obtained with a highly clinically relevant prostate cancer model, suggest, for the first time, that docetaxel-based therapy of advanced human prostate cancer may be improved by combining docetaxel with Aneustat.

© 2013 Federation of European Biochemical Societies. Published by Elsevier B.V. All rights reserved.

---

\* *Corresponding author.* Department of Experimental Therapeutics, BC Cancer Agency – Cancer Research Centre, 675 West 10th Avenue, Vancouver, BC, Canada V5Z 1L3. Tel.: +1 604 675 8013; fax: +1 604 675 8019.
E-mail addresses: siqu@bccrc.ca (S. Qu), kwang@prostatecentre.com (K. Wang), hxue@bccrc.ca (H. Xue), yuwang@bccrc.ca (Y. Wang), rwu@bccrc.ca (R. Wu), chengfei.liu@ucdmc.ucdavis.edu (A.C. Liu), acgao@ucdavis.edu (A.C. Gao), pgout@bccrc.ca (P.W. Gout), ccollins@prostatecentre.com (C.C. Collins), ywang@bccrc.ca (Y. Wang).

## 1. Introduction

Prostate cancer is the most commonly diagnosed non-cutaneous cancer and one of the leading causes of cancer death for North American men (Siegel et al., 2012). When the malignancy is localized to the prostate, surgery and radiation therapy can be curative. Many patients, however, will experience local recurrence and progression to metastasis (Fleshner, 2005). As prostate cancer growth in general is androgen-dependent, androgen ablation therapy of locally advanced, recurrent or metastatic prostate cancer is usually quite effective in the first 1—3 years. However, cancers frequently develop within 18—24 months into a more aggressive, presently incurable, androgen-independent phenotype, termed "castration-resistant prostate cancer" (CRPC) (Hotte and Saad, 2010). The emergence of CRPC typically manifests as rising serum prostate-specific antigen (PSA) levels (Oh and Kantoff, 1998). It is well established that the stimulation of PSA gene expression is mediated by the androgen receptor (AR), and increasing evidence suggests that the AR plays an important role in the development of CRPC (Chen et al., 2004; Mohler et al., 2004). Furthermore, there is an emerging role in the carcinogenesis and progression of prostate cancer for the PI3K/AKT pathway (Gao et al., 2012; Li et al., 2005), reported to be involved in cell migration, tissue invasion and therapy resistance of various types of cancer (Tian et al., 2010; Tokunaga et al., 2006).

The current standard first-line therapy for highly advanced metastatic prostate cancer is systemic docetaxel plus prednisone chemotherapy adopted in 2004 (McKeage, 2012). Docetaxel is a semi-synthetic, second-generation taxane derived from the bark of the European yew tree, Taxus baccata (Mangatal et al., 1989). Its main mode of anticancer action is based on interference with microtubule dynamics (assembly and disassembly) (Tabaczar et al., 2010), leading to inhibition of the progression of cells through the cell cycle (Garcia et al., 1994; Lavelle et al., 1995). Furthermore, docetaxel can induce cell apoptosis by altering the expression and phosphorylation of members of the Bcl-2 family of proteins (Pienta, 2001; Stein, 1999). However, treatment with docetaxel plus prednisone is not curative, is associated with severe side effects and increases the overall survival of patients only marginally when compared with the previous standard mitoxantrone plus prednisone regimen (Tannock et al., 2004).

New therapeutics have been developed, including Abiraterone acetate, a CYP17 inhibitor (de Bono et al., 2011), and Enzalutamide (formerly known as MDV3100), an AR inhibitor (Agarwal et al., 2012), that were approved by the US Food and Drug Administration (FDA) to treat metastatic CRPC patients who failed prior docetaxel-containing chemotherapy (Aragon-Ching, 2012; Logothetis et al., 2011). Various agents demonstrating additive or synergistic effects in preclinical studies have also been combined with docetaxel, but overall survival has so far not been extended compared to the docetaxel plus prednisone standard regimen (Antonarakis and Eisenberger, 2013; McKeage, 2012). Clearly, development of more effective drugs and novel therapeutic approaches are of critical importance for improving disease management and survival of metastatic prostate cancer patients.

Aneustat (OMN54) is a multifunctional/multitargeted botanical anti-cancer drug candidate (National Cancer Institute Drug Dictionary) developed by Omnitura Therapeutics Inc., USA. It is currently being evaluated in a Phase-I Clinical Trial in Canada (NCTId: NCT01555242). In a previous study in our laboratory, treatment with Aneustat alone suppressed the growth of subrenal LNCaP cell line xenografts markedly (Supplementary Figure S1). In the present study it was found that the combination of docetaxel and Aneustat can markedly and synergistically enhance anti-tumor activity in a metastatic prostate cancer tissue xenograft model derived from a patient's prostate cancer specimen (www.livingtumorlab.com). Expression microarray analysis indicated that the combined use of docetaxel and Aneustat led to expanded anticancer activity, in particular to targeting of pathways and cancer hallmarks, that was not attained when the drugs were used as single agents.

## 2. Materials and methods

### 2.1. Materials

Chemicals, solvents and solutions were obtained from Sigma—Aldrich, Oakville, ON, Canada, unless otherwise indicated. Aneustat was supplied by Omnitura Therapeutics Inc. (Henderson, NV) and docetaxel was purchased from Sanofi-Aventis Canada Inc. (Laval, Quebec, Canada).

### 2.2. Cell culture

Human C4-2 androgen-independent prostate cancer cells, i.e. metastatic, PTEN-deficient cells derived from the LNCaP cell line (Sobel and Sadar, 2005; Wu et al., 1998), were obtained from the Leland W. K. Chung Laboratory (Cedars-Sinai Medical Center). They were maintained as monolayer cultures in RPMI-1640 medium supplemented with fetal bovine serum (FBS; 10%), penicillin (100 units/ml) and streptomycin (100 $\mu$g/ml) at 37 °C in a humidified incubator with a 5% $CO_2$ atmosphere.

### 2.3. In vitro drug efficacy determination

Trypsinized C4-2 cells were seeded into 24-well culture plates (starting concentration approximately $1 \times 10^5$ cells/ml) and incubated at 37 °C in 5% $CO_2$ for 24 h. Aneustat and docetaxel (both dissolved in DMSO), were then added to the cultures as single drugs or in various combinations for a further 48-h incubation to assess the effects of the drugs on cell numbers; DMSO was used as a vehicle control.

### 2.4. Animals

Non-obese diabetic severe combined immunodeficiency (NOD-SCID) mice (males; 6—8 weeks old; body weight, 23—25 g), bred in the BC Cancer Research Centre ARC animal facility, were housed in sterile micro-isolator cages under specific pathogen-free conditions. Food and water were sterilized prior to use. Temperature (20—21 °C) and humidity (50—60%)

were controlled. Daily light cycles were 12 h light and 12 h dark. Cages were completely changed once or twice a week. Animals were handled under sterile conditions. The maximum tolerated dose of Aneustat was determined using conventional methodology. Animal care and experiments were carried out in accordance with the guidelines of the Canadian Council on Animal Care.

## 2.5. Prostate cancer xenograft model and treatment

The LTL-313H transplantable, PTEN-deficient, metastatic and PSA-secreting, patient-derived prostate cancer tissue line (Choi et al., 2012; Wu et al., 2012) (generation 13) was maintained as grafts under renal capsules of male NOD-SCID mice supplemented with testosterone as previously described (Watahiki et al., 2011). For experiments, tumors were harvested 10 weeks after grafting and pieces of tumor tissue (2.5 × 2.5 × 1.25 mm$^3$) were grafted under the renal capsules of 36 testosterone-supplemented male mice (6 groups; 6 mice/group; 4 grafts/mouse). The grafts had a 100% engraftment rate with an average tumor volume doubling time of 13−15 days. Increases in the plasma PSA levels of the mice were used as a measure of tumor growth. After about 6 weeks, when levels of ∼12 ng PSA/ml plasma had been reached, i.e. equivalent to tumor volumes of 30−50 mm$^3$, the mice were randomly distributed into 6 groups and treated with docetaxel (i.p.; Q7d/3) and Aneustat (orally; Q1d × 5/3) along the following schedule: (a) vehicle control, (b) docetaxel (5 mg/kg), (c) Aneustat (1652 mg/kg), (d) docetaxel (5 mg/kg) + Aneustat (413 mg/kg), (e) docetaxel (5 mg/kg) + Aneustat (826 mg/kg), and (f) docetaxel (5 mg/kg) + Aneustat (1652 mg/kg). After 3 weeks, the mice were euthanized, tumor volumes measured using callipers and tissue sections prepared for histopathological analysis (see below). Tumor growth of treated animals relative to untreated animals was used as a measure of antitumor activity, i.e. T/C = (treated tumor volume$_{3wks}$ − treated tumor volume$_{0wks}$):(control tumor volume$_{3wks}$ − control tumor volume$_{0wks}$) × 100%, with T/C > 0 indicating tumor growth and T/C < 0 indicating tumor shrinkage. Tumor growth inhibition = 100% − T/C.

## 2.6. Immunohistochemical staining

Preparation of paraffin-embedded tissue sections and immunohistochemical analyses were carried out as previously described (Wang et al., 2005b). The anti-Cleaved Caspase 3 (Asp175) (5A1E) (#9664, 1:50, rabbit anti-human; Cell Signaling Technology, Danvers, MA) was used for immunohistochemical staining. All sections used for immunohistochemistry were lightly counterstained with 5% (w/v) Harris hematoxylin. Five fields of each slide were randomly chosen and images taken (×400), using an AxioCam HR CCD mounted on an Axioplan 2 microscope and Axiovision 3.1 software (Carl Zeiss, Canada). Positively stained cells and whole cells in each image were counted and the percentage of positive cells was calculated. Caspase 3 expression could be used as an indicator of apoptotic activity since a high correlation was found between caspase 3 expression and apoptotic body counts (Supplementary Table S1).

## 2.7. Real-time PCR analysis

Total RNA was extracted using Trizol reagent (Invitrogen, Carlsbad, CA) according to the manufacturer's instructions. RNA (1 μg) extract was treated with DNase and reverse transcribed with random primers and Im-Prom II Reverse transcriptase (Promega, Madison, WI). The cDNA was subjected to quantitative real-time RT-PCR using specific primers for AR and β-actin. [AR: 5′-CCTGGCTTCCGCAACTTACAC, 3′-GGACTTGTGCATGCGGTACTCA, β-actin: 5′-CCCAGCCATGTACGTTGCTA, 3′-AGGGCATACCCCTCGTAGATG]. It was performed in 25 μl reaction mixtures using SYBR Green IQ supermix (Bio-Rad, Hercules, CA) according to the manufacturer's instructions. Expression levels of AR were normalized to β-actin. The experiment was performed three times in duplicate.

## 2.8. Western blot analysis

Whole cell and tissue protein extracts were resolved on SDS−PAGE using procedures previously reported (Nadiminty et al., 2008; Nakamura et al., 2011). Proteins were then transferred to nitrocellulose membrane. After blocking for 1 h at room temperature in 5% milk in PBS/0.1% Tween-20, membranes were incubated overnight at 4 °C with appropriate primary antibodies. Following incubation with secondary antibody, immunoreactive proteins were visualized with an enhanced chemiluminescence detection system (Amersham Pharmacia Biotech, Buckinghamshire, England). [AR (441) (sc-7305, mouse monoclonal antibody, Santa Cruz Biotechnology, Santa Cruz, CA); p-AKT1/2/3 (ser 473)-R (sc-7985-R, rabbit polyclonal antibody, Santa Cruz Biotechnology, Santa Cruz, CA); AKT (#9272, rabbit polyclonal antibody, Cell Signaling Technology); Bcl-2 (human specific) (#2872, rabbit polyclonal antibody, Cell Signaling Technology); Tubulin (T5168, Monoclonal Anti-α-Tubulin antibody, Sigma−Aldrich, St. Louis, MO)]. Tubulin was used to monitor the amounts of samples applied. The density of the blot bands was quantified using ImageJ software (National Institutes of Health, Bethesda, MD, USA; http://rsb.info.nih.gov/ij/).

## 2.9. Microarray analysis for gene expression profiles

Total RNA was extracted from xenograft tissues using a *mir*Vana™ miRNA Isolation Kit (Life Technologies, Burlington, ON, Canada) according to the manufacturer's instructions. The quality of the RNA was assessed with an Agilent 2100 bioanalyzer (Agilent, Santa Clara, CA); batches with an RNA integrity number value ≥8.0 were considered acceptable for microarray analysis. Samples were prepared following Agilent's One-Color Microarray-Based Gene Expression Analysis Low Input Quick Amp Labeling v6.0 (Agilent). An input of 100 ng of total RNA was used to generate cyanine-3-labeled cRNA. Samples were hybridized on Agilent SurePrint G3 Human GE 8 × 60K Microarray v2 (Design ID 039494). Then, arrays were scanned with the Agilent DNA Microarray Scanner at a 3 μm scan resolution and the data processed with Agilent Feature Extraction 11.0.1.1. Processed green signal was quantile normalized with Agilent GeneSpring 12.0. RNA quality control and microarray analysis were performed by the Laboratory for Advanced Genome Analysis at the Vancouver

Prostate Centre, Vancouver, Canada. All microarray profiling analyses were carried out in duplicate. The microarray gene expression data have been deposited in NCBI's Gene Expression Omnibus (GEO, www.ncbi.nlm.nih.gov/geo/) under accession number GSE48667.

## 2.10. Microarray data analysis

Microarray probe expression data were filtered for improved quality prior to downstream analysis. Specifically, probes without corresponding gene annotations and probes without detectable expression levels (less than 4 in log2 scale) were removed. Genes of treated tissues were considered differentially expressed relative to corresponding genes in non-treated, control tissues if their probes showed ≥2-fold difference. Pathway enrichment analysis was performed on such differentially expressed genes using Ingenuity Pathway Analysis software (IPA; Ingenuity Systems, Inc., Redwood City, CA). Statistical over-representation of canonical pathways in the drug-response-expression signatures was calculated using the Fischer's exact test and Benjamini-Hochberg (BH) multiple-test correction method (Savli et al., 2008; Solskov et al., 2012), and pathways with a BH-adjusted $p$-value<0.05 were considered significant. Differentially expressed genes in "docetaxel + Aneustat"-treated tissues, compared to controls, were linked to mechanism-based therapeutic targets, and the linkages of genes and functions were verified in the literature.

## 2.11. Statistics

Statistical analyses of gene expression data were performed as described above, otherwise the Student's $t$-test was used. Results were considered statistically significant when $p < 0.05$ and are expressed as means ± SEM.

## 3. Results

### 3.1. Effects of Aneustat, docetaxel and combinations of the drugs on growth of human C4-2 prostate cancer cell cultures

As shown in Figure 1A and B, Aneustat markedly inhibited C4-2 cell population growth in a dose-dependent manner, showing inhibitions at hr 48 of 42% and 83% at concentrations of 50 and 100 μg/ml, respectively ($p < 0.05$). Docetaxel at 1 nM had only a minor effect on C4-2 culture growth, showing an inhibition of 21%. Combinations of docetaxel (1 nM) + Aneustat (50 μg/ml) and docetaxel (1 nM) + Aneustat (100 μg/ml) led to growth inhibitions of 63% and 93%, respectively ($p < 0.05$), indicating that the growth inhibitions of the drug combinations were essentially additive in nature.

### 3.2. Effects of docetaxel + Aneustat on growth of LTL-313H prostate cancer xenografts: synergistic growth inhibition

In preliminary experiments it was found that the maximum tolerated dose of orally administered Aneustat (used in combination with docetaxel) was 1652 mg/kg body weight for NOD-SCID mice at Q1d × 5/3.

Groups of NOD-SCID mice bearing LTL-313H xenografts with an average tumor volume of about 32 mm³ (as indicated by plasma PSA levels) were treated for 3 weeks with docetaxel and Aneustat as single agents and with combinations of the two drugs, using a fixed sub-therapeutic dosage of docetaxel (5 mg/kg body weight) and increasing dosages of Aneustat (see Figure 2). The final average tumor volume in the control group was 133 ± 21 mm³ (mean ± SEM). Treatment of the mice with Aneustat (1652 mg/kg), the maximum tolerated
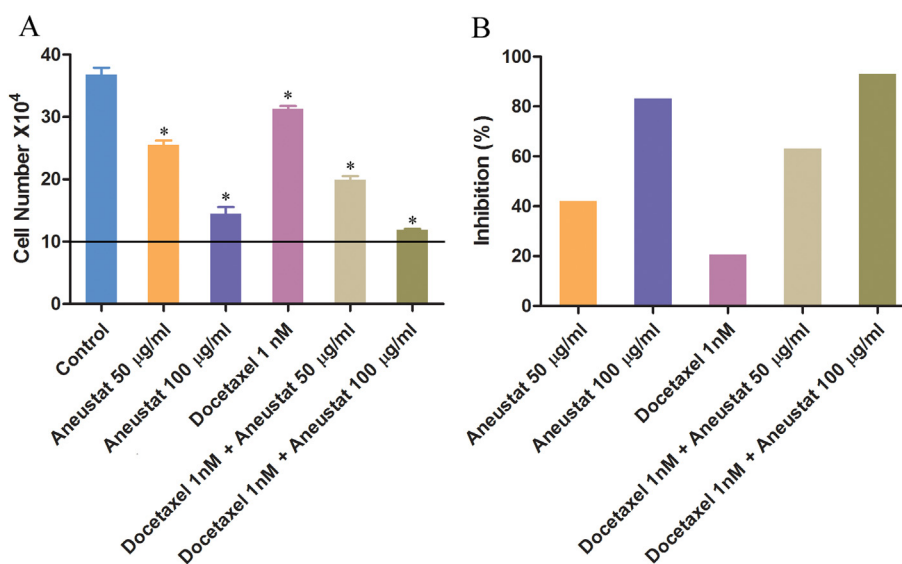


Figure 1 − Effects of Aneustat, docetaxel and docetaxel + Aneustat on the growth of human C4-2 prostate cancer cell cultures. Cells were incubated for 48 h with Aneustat and docetaxel at the concentrations and combinations indicated; initial cell concentration, $10 \times 10^4$ cells/ml, as indicated by the horizontal line. (A) Cell population at 48 h. The asterisk indicates $p < 0.05$ (relative to control). (B) Percentage growth inhibition relative to control.

dose, inhibited tumor growth by 30% ($p = 0.19$). Treatment with docetaxel (5 mg/kg) inhibited tumor growth by 51% ($p < 0.05$). Aneustat significantly increased the growth-inhibitory effect obtained with 5 mg/kg docetaxel in a dose-dependent fashion to 81%, 100% and 106%, at Aneustat dosages of 413, 826 and 1652 mg/kg, respectively ($p < 0.05$). The combination of docetaxel and the highest dosage of Aneustat (1652 mg/kg) caused complete growth inhibition coupled to significant tumor volume shrinkage ($p < 0.05$) with a T/C value of −6.1% (Figure 2). The data indicate that Aneustat enhanced the anticancer *in vivo* effect of docetaxel in a synergistic fashion. No major change in appearance and behavior of the animals was observed during the experiments, nor significant organ damage at the endpoint, indicating that the treatments were quite well tolerated by the tumor-bearing mice.

### 3.3.  Docetaxel + Aneustat treatment leads to increased apoptosis in LTL-313H xenografts

Histopathological analysis of H&E-stained tumor tissue sections (Figure 3A—D) showed regular mitotic activity in the control tumors as well as sporadic areas of local necrosis, presumably due to the fast growth of the tumors. The tumors treated with Aneustat or docetaxel as single agents showed elevated numbers of cells arrested in the early phase of mitosis. In contrast, the tumors treated with both docetaxel and the highest Aneustat dosage (1652 mg/kg) exhibited higher amounts of stroma and necrosis area, but few cells could be seen in mitosis.

Caspase 3 expression, used as an indicator of apoptotic activity (Figure 3E—H), indicated that docetaxel and Aneustat alone, or docetaxel in combination with the low and medium dosages of Aneustat, only slightly increased apoptosis; in contrast, docetaxel in combination with the highest Aneustat
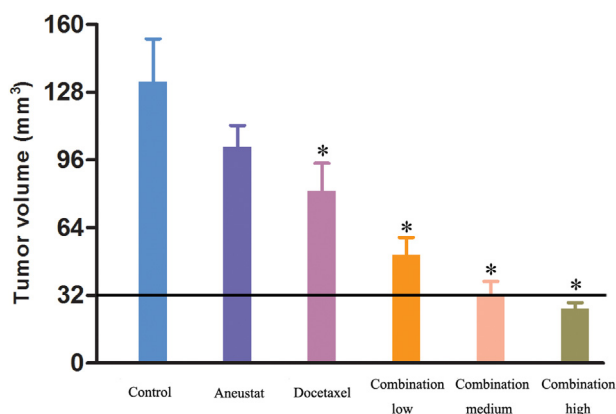


**Figure 2 − Effects of a 3-week treatment with Aneustat, docetaxel, and combinations of the two drugs, on the growth of LTL-313H prostate cancer xenografts. The average volume of the xenografts at the start of treatment was approximately 32 mm$^3$ (indicated by the horizontal line). Control (DMSO); Aneustat (1652 mg/kg; Q1d × 5/3); Docetaxel (5 mg/kg; i.p., Q7d/3); Combination low, docetaxel (5 mg/kg) + Aneustat (413 mg/kg); Combination medium, docetaxel (5 mg/kg) + Aneustat (826 mg/kg); Combination high, docetaxel (5 mg/kg) + Aneustat (1652 mg/kg). Data are presented as tumor volume (mean ± SEM). The asterisks indicate $p < 0.05$ relative to control.**

dosage substantially enhanced caspase-dependent apoptosis relative to the control (207%) and to apoptosis induced by docetaxel alone (117%) (Figure 3I; $p < 0.05$).

### 3.4.  Aneustat inhibits AR expression and AKT phosphorylation in C4-2 cells; synergistic effect of docetaxel + Aneustat in LTL-313H xenografts

We investigated the effect of the drugs on expression of AR, a major factor in prostate cancer growth (Heinlein and Chang, 2004) and on AKT signaling which plays a critical role in the progression of the disease (Sarker et al., 2009). As shown in Figure 4A, AR mRNA expression in C4-2 cells was markedly inhibited by Aneustat (≥100 μg/ml). Densitometric analysis using ImageJ software of Western blot bands (Figure 4B) showed that Aneustat caused decreases of 53, 76 and 86% in the AR expression of C4-2 cells, compared with controls, at dosages of 50, 100 and 200 μg/ml, respectively. Similarly, Aneustat inhibited the phosphorylation of AKT by 63 and 89% at dosages of 100 and 200 μg/ml, respectively, as distinct from the amount of AKT (Figure 4B). A marked effect of Aneustat on Bcl-2 expression, an anti-apoptotic protein that plays a role in the PI3K/AKT pathway was found only at a concentration of 200 μg/ml, i.e. 85% inhibition (Figure 4B).

As shown by Western blot and densitometric analysis (Figure 4C), treatment of LTL-313H xenografts with Aneustat alone (1652 mg/kg) did not affect AR expression, but slightly down-regulated AKT phosphorylation (23%). Treatment with docetaxel alone (5 mg/kg) down-regulated both AR expression and AKT phosphorylation by 33 and 44%, respectively. However, the combination of docetaxel (5 mg/kg) and Aneustat (1652 mg/kg) markedly inhibited both AR expression (77%) and AKT phosphorylation (69%) (without affecting the amount of AKT), indicative of synergistic action of the two drugs.

### 3.5.  Treatment of LTL-313H xenografts with docetaxel, Aneustat and docetaxel + Aneustat: mechanisms of action indicated by DNA microarray data analysis

Expression microarray data were obtained from LTL-313H xenografts treated for 3 weeks with docetaxel (5 mg/kg), Aneustat (1652 mg/kg) and docetaxel (5 mg/kg) + Aneustat (1652 mg/kg), and from untreated controls. Genes showing significant differential expression (with ≥2-fold difference) between untreated and treated xenografts were used for pathway analysis using Ingenuity Pathway Analysis (IPA) software. The results indicate that both single drugs and combined drugs can act through inhibition or stimulation of canonical pathways (see Table 1). For example, docetaxel can inhibit cell cycling and promote apoptosis (by boosting p53 signaling), consistent with established observations (Li et al., 2004). Aneustat, used as a single drug, stimulates LXR/RXR activation and serotonin degradation, inhibits cell cycling and promotes apoptosis. The combination of 'docetaxel + Aneustat' can affect pathways induced by the drugs acting as single agents, such as inhibition of IGF-1 signaling by docetaxel, or stimulation of LXR/RXR activation by Aneustat. But more importantly, it can also act on pathways not observably influenced by the drugs used as single

agents, such as the metabolic pathways of cholesterol biosynthesis, glycolysis I and gluconeogenesis I.

### 3.6. Docetaxel + Aneustat treatment of LTL-313H xenografts affects genes involved in cancer hallmarks

Genes showing significant (≥2-fold) changes in expression in response to treatment of the xenografts with 'docetaxel + Aneustat' were categorized based on their roles in the hallmarks of cancer. Figure 5A shows that the combined drug treatment affects most major aspects of cancer development. Thus the drug combination down-regulated genes promoting cell proliferation, facilitating cell invasion and metastasis, inducing angiogenesis and enhancing aerobic glycolysis; it up-regulated genes promoting cell apoptosis. Figure 5B shows a down-regulatory effect of the combined drug treatment on the expression of genes involved in aerobic glycolysis, a major hallmark of cancer (Vander Heiden et al., 2009). A comprehensive list of differentially expressed genes is presented in the Supplementary Table S2.

## 4. Discussion

The present study was aimed at determining, in preclinical studies, whether the efficacy of docetaxel-based prostate cancer therapy could be enhanced by combining docetaxel with Aneustat (OMN54), a multivalent botanical drug candidate that is currently assessed in a Phase-I Clinical Trial (NCTId: NCT01555242). Although docetaxel-based therapy currently represents the best available treatment for highly advanced metastatic prostate cancer, it only marginally extends patients' lives (McKeage, 2012; Tannock et al., 2004). Drug development efforts have therefore focussed on improvement of its efficacy by combining docetaxel with a wide variety of anticancer agents. However, as recently pointed out in an editorial (Antonarakis and Eisenberger, 2013), Phase III clinical trials using docetaxel-based combinations for metastatic castration-resistant prostate cancer have so far failed to demonstrate an improvement in patient survival, in spite of indications by preclinical studies that the efficacy of docetaxel was enhanced by the drug combinations. Such a discrepancy between drug efficacies established in the clinic and those predicted by preclinical studies is very evident for new, potential anticancer agents. Thus only ~5% of anticancer drug candidates, that have successfully passed required preclinical in vivo efficacy screening tests, have significant effectiveness in clinical trials and are approved for clinical usage by the U.S. Food & Drug Administration (Kummar et al., 2007; Sharpless and Depinho, 2006). It has become apparent that preclinical assessment of clinical efficacy of anticancer drugs is seriously hampered by a lack of
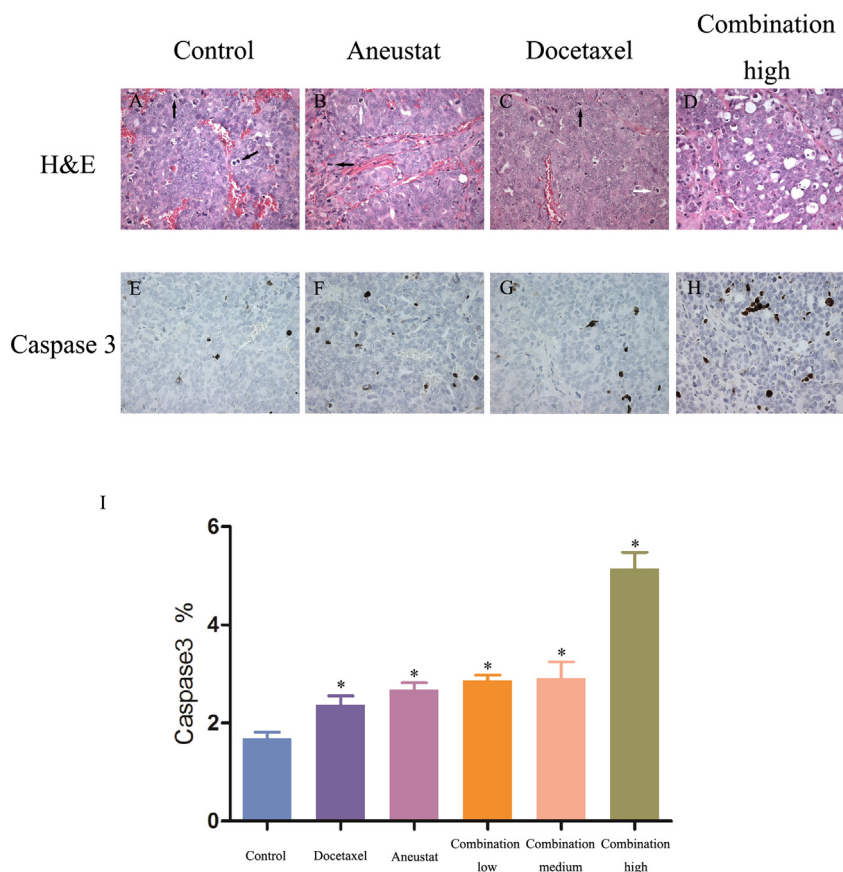


Figure 3 — Effects of a 3-week treatment with Aneustat and docetaxel, used as single agents or in combination (see legend Fig. 2), on apoptosis in LTL-313H xenografts as revealed by caspase 3 expression. A—D: tissue sections stained with H&E, black arrows point at mitotic figures, white arrows point at dying cells; E—H: tissue sections stained for caspase 3; magnification × 400. I: Relative caspase 3 expression (means ± SEM). The asterisks indicate $p < 0.05$ relative to control.

clinically relevant, experimental *in vivo* cancer models. Subcutaneous cancer *cell line* xenograft models, commonly used for preclinical *in vivo* drug efficacy tests, do not adequately predict the efficacy of anticancer agents in the clinic (Johnson et al., 2001; Kamb, 2005; Leaf, 2004; Sharpless and Depinho, 2006). To assess the effect of combining docetaxel with Aneustat, we therefore did not only make use of C4-2 cell cultures, but especially of NOD-SCID mice carrying xenografts of a transplantable LTL-313H prostate cancer *tissue* xenograft line. This metastatic, PTEN-deficient, PSA-secreting line was developed from a patient's primary prostatic adenocarcinoma (Watahiki et al., 2011), using subrenal capsule grafting

**Figure 4 − Effect of Aneustat and docetaxel on AR expression and AKT phosphorylation. (A) Effect of a 24-h treatment of C4-2 cell cultures with Aneustat on AR mRNA expression (by qPCR) and (B) on AR protein expression, AKT phosphorylation and amount of AKT. (C) Effect of a 3-week treatment of LTL-313H xenografts with Aneustat (1652 mg/kg), docetaxel (5 mg/kg) and a combination of docetaxel (5 mg/kg) + Aneustat (1652 mg/kg) on AR protein expression, AKT phosphorylation and amount of AKT.**

technology that tends to preserve important properties of the original cancers, including histopathology, chromosomal aberrations, gene expression profiles and 3-dimensional architecture of the malignancy (Collins et al., 2012; Tung et al., 2011; Wang et al., 2005a, 2005b) thus rendering high clinical relevance to this advanced prostate cancer model. The use of this model in the present study therefore increases the likelihood that the results obtained are useful.

In contrast to the marked inhibitory effect of Aneustat alone on the replication of C4-2 cells *in vitro* (Figure 1), the treatment of LTL-313H xenografts with Aneustat alone during a 3-week period (dosage: 1652 mg/kg at Q1d × 5/3) was not statistically significant (Figure 2). However, the combination of Aneustat with docetaxel (5 mg/kg) markedly increased the inhibition of the growth of xenografts obtained with docetaxel alone (Figure 2). Even the lowest *in vivo* dosage of Aneustat (413 mg/kg), used in combination with docetaxel, resulted in a 30% increase in the growth-inhibitory effect obtained with docetaxel alone ( $p < 0.05$; Figure 2). The synergistic enhancement of anticancer activity by the combination of docetaxel and Aneustat is particularly evident from the complete inhibition of the growth of the LTL-313H xenografts and their shrinkage (T/C = −6.1%) resulting from treatment with Aneustat (at 1652 mg/kg) in combination with docetaxel used at 5 mg/kg body weight, a sub-therapeutic dosage (Figure 2). The tumor shrinkage was associated with an increase in apoptotic activity (Figure 3H,I), an effect not observed when docetaxel or Aneustat were used as single agents (Figure 3I). Importantly, the combination of docetaxel and Aneustat was quite well tolerated by the animals. The data suggest that docetaxel-based treatment of advanced prostate cancer may be enhanced by using docetaxel in combination with Aneustat.

It is not clear why Aneustat and docetaxel had synergistic growth-inhibitory effects *in vivo*, but not *in vitro* (Figures 1 and 2). The synergism of the drugs *in vivo* may be a reflection of the much greater biological complexity of the *in vivo* situation, including the presence of a variety of host cells and organs that could modulate the actions of the drugs and their interactions with target cells.

The mechanism by which the combination of docetaxel and Aneustat enhances the anticancer activity *in vivo* is of major interest for potential improvement of docetaxel-based therapy of advanced prostate cancer. Its elucidation requires an understanding of the molecular actions of both drugs, in particular when they are used in combination. Docetaxel is well known for its interference with microtubule assembly/disassembly to cause growth arrest and induction of apoptosis (Pienta, 2001; Stein, 1999; Tabaczar et al., 2010), as also observed in the present study using LTL-313H prostate cancer xenografts (Figures 2 and 3). These mechanisms of docetaxel action are confirmed in our gene expression profiling analysis of the docetaxel-treated xenografts (Table 1), indicating that the reductive effects of docetaxel on the xenografts are based on inhibition of cyclins and cell cycle regulation and also on stimulation of p53 signaling, a process that may lead to apoptosis (Liu et al., 2013). Furthermore, it has been reported that docetaxel can down-regulate AR expression in prostate cancer (Kuroda et al., 2009), an observation which was confirmed in the present study (Figure 4C).
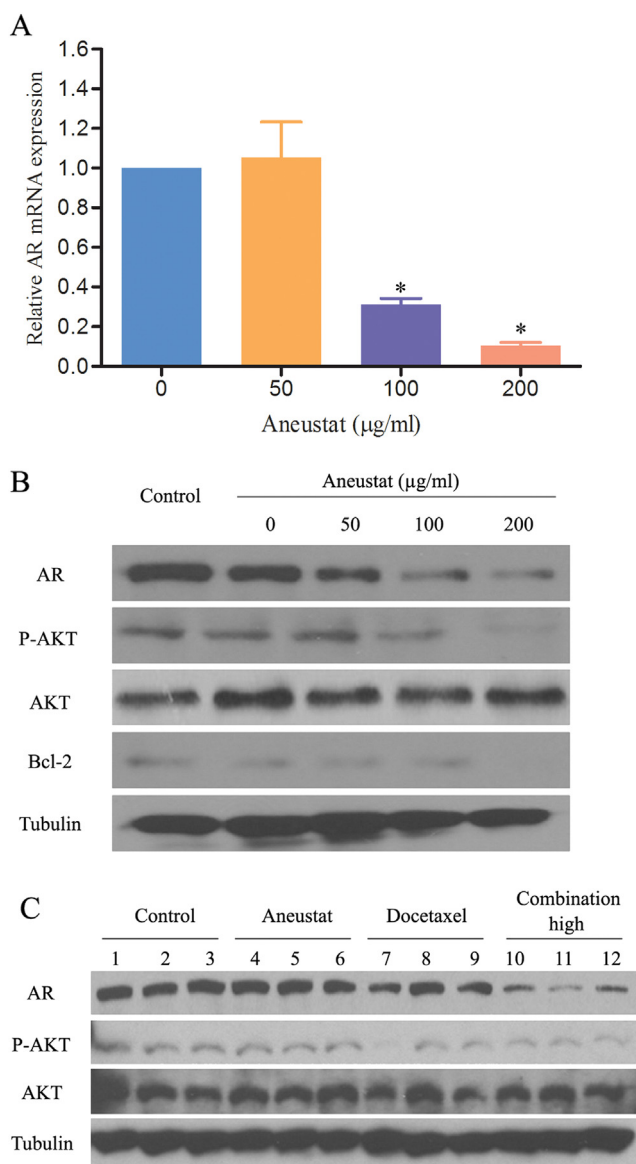
**Table 1 — Pathways stimulated (↑) or inhibited (↓) in LTL-313H xenografts by treatment with docetaxel (5 mg/kg), Aneustat (1652 mg/kg) and docetaxel + Aneustat as predicted by Ingenuity Pathway Analysis of DNA microarray data.**

| Pathways | Docetaxel | Aneustat | Combination |
|---|---|---|---|
| Mitotic roles of polo-like Kinase | − | − | ↓ |
| Cell cycle control of chromosomal replication | − | − | ↓ |
| ATM signaling | − | − | ↓ |
| Role of CHK proteins in cell cycle checkpoint control | − | − | ↓ |
| LXR/RXR activation | − | ↑ | ↑ |
| Serotonin degradation | − | ↑ | − |
| Cyclins and cell cycle regulation | ↓ | ↓ | ↓ |
| GADD45 signaling | ↑ | ↑ | ↑ |
| Cholesterol biosynthesis | − | − | ↓ |
| Glycolysis I | − | − | ↓ |
| Gluconeogenesis I | − | − | ↓ |
| Cell Cycle: G1/S checkpoint regulation | ↓ | ↓ | ↓ |
| p53 signaling | ↑ | ↑ | ↑ |
| Mitochondrial dysfunction | ↓ | ↓ | ↓ |
| IL-8 signaling | ↓ | ↓ | ↓ |
| IGF-1 signaling | ↓ | − | ↓ |
| ILK signaling | ↓ | − | − |

There is currently no published information regarding the molecular mechanisms of action of Aneustat. Our study indicates — for the first time — that Aneustat can induce apoptosis (Figure 3), as well as inhibit AR expression, AKT phosphorylation and Bcl-2 expression (Figure 4), processes that play important roles in the malignant progression of prostate cancer and its chemoresistance (Guyader et al., 2012; Mulholland et al., 2006; Xin et al., 2006). The gene expression profiling of Aneustat-treated xenografts (Table 1) suggests stimulation of LXR/RXR activation as an action of Aneustat. This suggestion is supported by the finding that Aneustat reduced AKT phosphorylation of C4-2 prostate cancer cells (Figure 4B), as LXR activation has been reported to down-regulate AKT phosphorylation in prostate cancer cells (Pommier et al., 2010). The gene expression analysis also suggests stimulation of serotonin degradation as another action of Aneustat (Table 1). Studies have shown that growth of prostate cancer cells can be interrupted by inhibiting the synthesis and metabolism of serotonin, a neurotransmitter that plays a role as a growth factor for prostate cancer cells (Dizeyi et al., 2011; Shinka et al., 2011). Additional experimental verification will be needed to establish these mechanistic properties of Aneustat. It may be noted that although Aneustat on its own did not significantly inhibit the growth of the LTL-313H cancer tissue xenografts that were grafted under renal capsules, it markedly suppressed the growth of e.g., subrenal LNCaP cell line xenografts (Supplementary Figure S1), consistent with the growth-inhibitory effects of Aneustat on C4-2 cells in vitro

(Figure 1). Further studies are needed to determine the basis of these differences in the in vivo growth-inhibitory activities of Aneustat.

Notably, treatment of the prostate cancer xenografts with the 'docetaxel + Aneustat' combination inhibited critical cancer pathways that were not affected by the individual drugs, such as cholesterol biosynthesis, glycolysis I and gluconeogenesis (Table 1). Cholesterol has an emerging role in prostate cancer as a potential therapeutic target, as intracellular cholesterol has recently been found to promote prostate cancer progression through regulation of AKT signaling and as a substrate for de novo androgen synthesis (Lee et al., 2013; Pelton et al., 2012). The inhibitions of glycolysis I and gluconeogenesis I are of special interest, since these two pathways have important roles in "reprogrammed energy metabolism", a key hallmark of cancer (Hanahan and Weinberg, 2011). Expression microarray profiling of the xenografts confirmed that the majority of the genes involved in the glycolysis pathway were indeed down-regulated by the docetaxel + Aneustat treatment (Figure 5B). Taken together, the data suggest that the increased anti-tumor activity of the docetaxel + Aneustat combination is based on an expansion of anticancer activity, targeting multiple pathways and hallmarks of cancer, not attainable with the single drugs.

The effect of docetaxel + Aneustat on glycolysis is of major interest, since treatment with this drug combination could lead to a reduction in lactic acid secretion by cancers. As recently reviewed by us (Choi et al., 2013), there is increasing evidence that cancer cells can suppress the anticancer immune response through maintaining a relatively low pH in their micro-environment via regulation of their lactic acid secretion. They are thought to achieve this via modification of glucose/glutamine metabolisms. Treatment targeting these metabolisms could reduce lactic acid secretion of cancers and increase the pH of the tumor micro-environment to more normal levels. This would lead to restoration of the local anticancer immune response. It appears from these considerations that treatment with docetaxel + Aneustat could not only affect cancers by direct drug-cancer cell interactions, but also indirectly, i.e. in immuno-competent hosts, through restoring the immune response in the cancer micro-environment.

It is generally accepted that cancers have an ability to circumvent therapy by switching from a targeted pathway to a different one (Hanahan and Weinberg, 2011). The combination of docetaxel + Aneustat may also interfere with this process by targeting multiple aspects of cancer (Figure 5, Table 1) and hence reduce the probability for the disease to evade a particular therapeutic approach by switching to other pathways.

AR and AKT signaling are important processes underlying prostate cancer growth (Xin et al., 2006). Inhibition of both AR expression and AKT signaling is apparently required to obtain near-complete regression of PTEN-deficient prostate cancers (Carver et al., 2011; Oh et al., 2012). The LTL-313H xenograft tissue line used in this study is deficient in PTEN (Wu et al., 2012) and the finding that treatment of the xenografts with docetaxel + Aneustat, as distinct from the single agents, led to complete inhibition of tumor growth coupled to tumor shrinkage, is consistent with inhibition of both
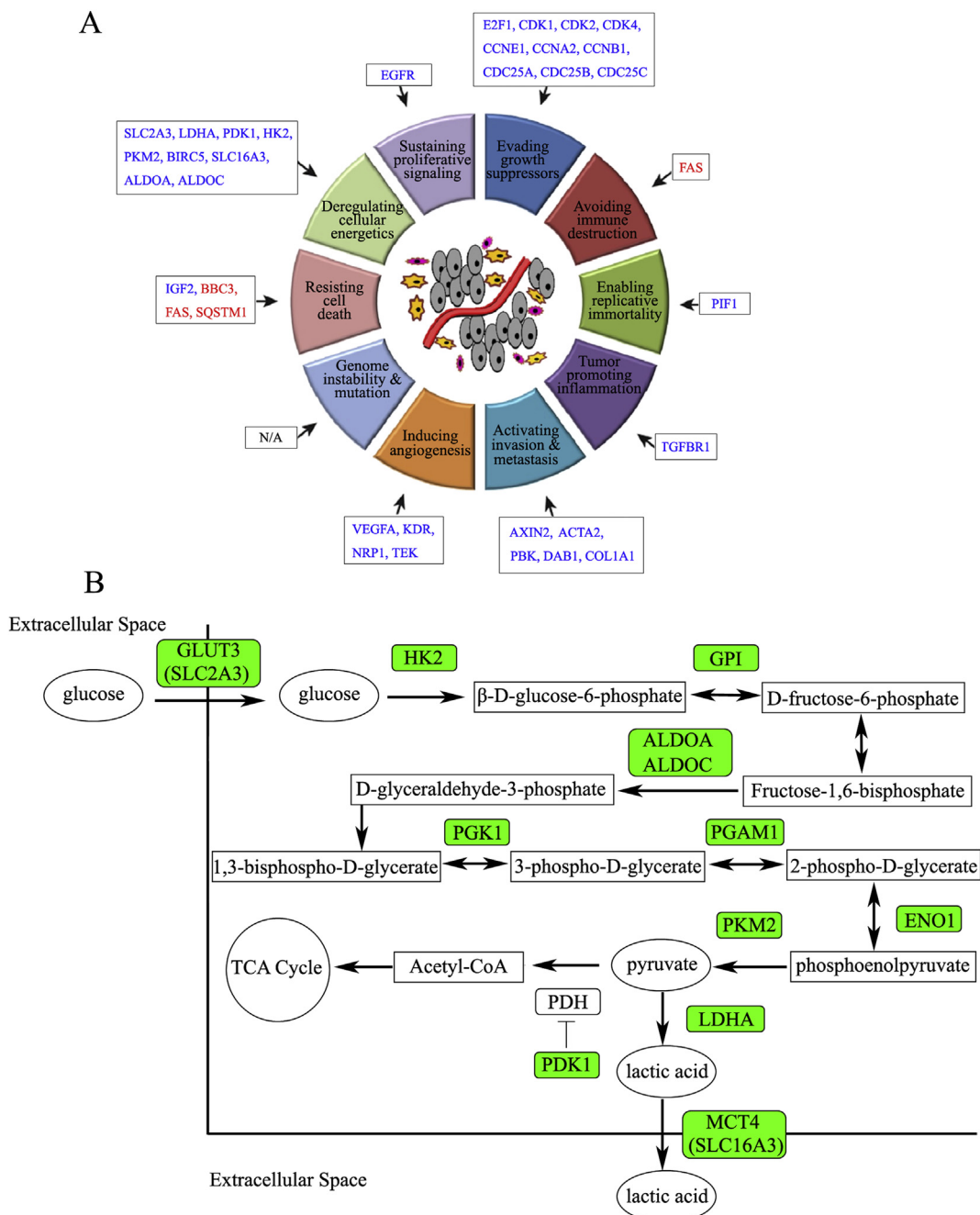
Figure 5 — Effects of treatment of LTL-313H xenografts with docetaxel + Aneustat on expression of cancer hallmark-mediating genes as revealed via DNA microarray analysis. (A) Up-regulated (red) and down-regulated (blue) genes. (B) Down-regulated (green) glycolysis-associated genes. Additional information is presented in the Supplementary Table S2.

AR expression and AKT phosphorylation in xenografts obtained only in the case of the combined drug treatment (Figure 4C).

In conclusion, the present study has shown, for the first time, that the combination of docetaxel and Aneustat can markedly and synergistically enhance the anticancer activity in a highly clinically relevant advanced prostate cancer model. The enhanced efficacy appears to be based on expanded anticancer activity, targeting multiple pathways and hallmarks of cancer, which results from the combination of docetaxel and Aneustat. The data suggest that docetaxel-based therapy of advanced human prostate cancer may be improved by using docetaxel in combination with Aneustat.

## Grant support

## Disclosure of potential conflicts of interest

## Author contributions

- Conception, design and study supervision: Yuzhuo Wang.
- Development of methodology: Hui Xue, Yuwei Wang, Rebecca Wu, Sifeng Qu, Chengfei Liu.
- Acquisition of data: Hui Xue, Yuwei Wang, Sifeng Qu, Rebecca Wu, Chengfei Liu.
- Analysis and interpretation of data: Sifeng Qu, Kendric Wang.
- Writing of the manuscript: Sifeng Qu, Peter Gout, Kendric Wang, Colin C. Collins, Allen C. Gao, Yuzhuo Wang.

## Acknowledgments

## Appendix A.
## Supplementary data

Supplementary data related to this article can be found at http://dx.doi.org/10.1016/j.molonc.2013.12.004.

REFERENCES

Agarwal, N., Sonpavde, G., Sternberg, C.N., 2012. Novel molecular targets for the therapy of castration-resistant prostate cancer. Eur. Urol. 61, 950–960.
Antonarakis, E.S., Eisenberger, M.A., 2013. Phase III trials with docetaxel-based combinations for metastatic castration-resistant prostate cancer: time to learn from past experiences. J. Clin. Oncol. 31, 1709–1712.
Aragon-Ching, J.B., 2012. Enzalutamide (formerly MDV3100) as a new therapeutic option for men with metastatic castration-resistant prostate cancer. Asian J. Androl. 14, 805–806.
Carver, B.S., Chapinski, C., Wongvipat, J., Hieronymus, H., Chen, Y., Chandarlapaty, S., Arora, V.K., Le, C., Koutcher, J., Scher, H., Scardino, P.T., Rosen, N., Sawyers, C.L., 2011. Reciprocal feedback regulation of PI3K and androgen receptor signaling in PTEN-deficient prostate cancer. Cancer Cell 19, 575–586.
Chen, C.D., Welsbie, D.S., Tran, C., Baek, S.H., Chen, R., Vessella, R., Rosenfeld, M.G., Sawyers, C.L., 2004. Molecular

determinants of resistance to antiandrogen therapy. Nat. Med. 10, 33–39.
Choi, S.Y., Collins, C.C., Gout, P.W., Wang, Y., 2013. Cancer-generated lactic acid: a regulatory, immunosuppressive metabolite? J. Pathol. 230, 350–355.
Choi, S.Y., Gout, P.W., Collins, C.C., Wang, Y., 2012. Epithelial immune cell-like transition (EIT): a proposed transdifferentiation process underlying immune-suppressive activity of epithelial cancers. Differentiation 83, 293–298.
Collins, C.C., Volik, S.V., Lapuk, A.V., Wang, Y., Gout, P.W., Wu, C., Xue, H., Cheng, H., Haegert, A., Bell, R.H., Brahmbhatt, S., Anderson, S., Fazli, L., Hurtado-Coll, A., Rubin, M.A., Demichelis, F., Beltran, H., Hirst, M., Marra, M., Maher, C.A., Chinnaiyan, A.M., Gleave, M., Bertino, J.R., Lubin, M., 2012. Next generation sequencing of prostate cancer from a patient identifies a deficiency of methylthioadenosine phosphorylase, an exploitable tumor target. Mol. Cancer Ther. 11, 775–783.
de Bono, J.S., Logothetis, C.J., Molina, A., Fizazi, K., North, S., Chu, L., Chi, K.N., Jones, R.J., Goodman, O.B., Saad, F., Staffurth, J.N., Mainwaring, P., Harland, S., Flaig, T.W., Hutson, T.E., Cheng, T., Patterson, H., Hainsworth, J.D., Ryan, C.J., Sternberg, C.N., Ellard, S.L., Fléchon, A., Saleh, M., Scholz, M., Efstathiou, E., Zivi, A., Bianchini, D., Loriot, Y., Chieffo, N., Kheoh, T., Haqq, C.M., Scher, H.I., Investigators, C.-A., 2011. Abiraterone and increased survival in metastatic prostate cancer. N. Engl. J. Med. 364, 1995–2005.
Dizeyi, N., Hedlund, P., Bjartell, A., Tinzl, M., Austild-Taskén, K., Abrahamsson, P.A., 2011. Serotonin activates MAP kinase and PI3K/Akt signaling pathways in prostate cancer cell lines. Urol. Oncol. 29, 436–445.
Fleshner, N., 2005. Defining high-risk prostate cancer: current status. Can J. Urol. 12 (Suppl. 1), 14–17. Discussion 94-16.
Gao, M., Patel, R., Ahmad, I., Fleming, J., Edwards, J., McCracken, S., Sahadevan, K., Seywright, M., Norman, J., Sansom, O., Leung, H.Y., 2012. SPRY2 loss enhances ErbB trafficking and PI3K/AKT signalling to drive human and mouse prostate carcinogenesis. EMBO Mol. Med. 4, 776–790.
Garcia, P., Braguer, D., Carles, G., el Khyari, S., Barra, Y., de Ines, C., Barasoain, I., Briand, C., 1994. Comparative effects of taxol and taxotere on two different human carcinoma cell lines. Cancer Chemother. Pharmacol. 34, 335–343.
Guyader, C., Céraline, J., Gravier, E., Morin, A., Michel, S., Erdmann, E., de Pinieux, G., Cabon, F., Bergerat, J.P., Poupon, M.F., Oudard, S., 2012. Risk of hormone escape in a human prostate cancer model depends on therapy modalities and can be reduced by tyrosine kinase inhibitors. PLoS One 7, e42252.
Hanahan, D., Weinberg, R.A., 2011. Hallmarks of cancer: the next generation. Cell 144, 646–674.
Heinlein, C.A., Chang, C., 2004. Androgen receptor in prostate cancer. Endocr. Rev. 25, 276–308.
Hotte, S.J., Saad, F., 2010. Current management of castrate-resistant prostate cancer. Curr. Oncol. 17 (Suppl. 2), S72–S79.
Johnson, J.I., Decker, S., Zaharevitz, D., Rubinstein, L.V., Venditti, J.M., Schepartz, S., Kalyandrug, S., Christian, M., Arbuck, S., Hollingshead, M., Sausville, E.A., 2001. Relationships between drug activity in NCI preclinical in vitro and in vivo models and early clinical trials. Br. J. Cancer 84, 1424–1431.
Kamb, A., 2005. What's wrong with our cancer models? Nat. Rev. Drug Discov. 4, 161–165.
Kummar, S., Kinders, R., Rubinstein, L., Parchment, R.E., Murgo, A.J., Collins, J., Pickeral, O., Low, J., Steinberg, S.M., Gutierrez, M., Yang, S., Helman, L., Wiltrout, R., Tomaszewski, J.E., Doroshow, J.H., 2007. Compressing drug development timelines in oncology using phase '0' trials. Nat. Rev. Cancer 7, 131–139.
Kuroda, K., Liu, H., Kim, S., Guo, M., Navarro, V., Bander, N.H., 2009. Docetaxel down-regulates the expression of androgen

receptor and prostate-specific antigen but not prostate-specific membrane antigen in prostate cancer cell lines: implications for PSA surrogacy. Prostate 69, 1579–1585.

Lavelle, F., Bissery, M.C., Combeau, C., Riou, J.F., Vrignaud, P., André, S., 1995. Preclinical evaluation of docetaxel (Taxotere). Semin. Oncol. 22, 3–16.

Leaf, C., 2004. Why we're losing the war on cancer (and how to win it). Fortune 149, 76–82, 84–76, 88 passim.

Lee, B.H., Taylor, M.G., Robinet, P., Smith, J.D., Schweitzer, J., Sehayek, E., Falzarano, S.M., Magi-Galluzzi, C., Klein, E.A., Ting, A.H., 2013. Dysregulation of cholesterol homeostasis in human prostate cancer through loss of ABCA1. Cancer Res. 73, 1211–1218.

Li, L., Ittmann, M.M., Ayala, G., Tsai, M.J., Amato, R.J., Wheeler, T.M., Miles, B.J., Kadmon, D., Thompson, T.C., 2005. The emerging role of the PI3-K-Akt pathway in prostate cancer progression. Prostate Cancer Prostatic Dis. 8, 108–118.

Li, Y., Li, X., Hussain, M., Sarkar, F.H., 2004. Regulation of microtubule, apoptosis, and cell cycle-related genes by taxotere in prostate cancer cells analyzed by microarray. Neoplasia 6, 158–167.

Liu, C., Zhu, Y., Lou, W., Nadiminty, N., Chen, X., Zhou, Q., Shi, X.B., deVere White, R.W., Gao, A.C., 2013. Functional p53 determines docetaxel sensitivity in prostate cancer cells. Prostate 73, 418–427.

Logothetis, C.J., Efstathiou, E., Manuguid, F., Kirkpatrick, P., 2011. Abiraterone acetate. Nat. Rev. Drug Discov. 10, 573–574.

Mangatal, L., Adeline, M., Guénard, D., Guéritte-Voegelein, F., Potier, P., 1989. Application of the vicinal oxyamination reaction with asymmetric induction to the hemisynthesis of taxol and analogues. Tetrahedron 45, 4177–4190.

McKeage, K., 2012. Docetaxel: a review of its use for the first-line treatment of advanced castration-resistant prostate cancer. Drugs 72, 1559–1577.

Mohler, J.L., Gregory, C.W., Ford, O.H., Kim, D., Weaver, C.M., Petrusz, P., Wilson, E.M., French, F.S., 2004. The androgen axis in recurrent prostate cancer. Clin. Cancer Res. 10, 440–448.

Mulholland, D.J., Dedhar, S., Wu, H., Nelson, C.C., 2006. PTEN and GSK3beta: key regulators of progression to androgen-independent prostate cancer. Oncogene 25, 329–337.

Nadiminty, N., Chun, J.Y., Lou, W., Lin, X., Gao, A.C., 2008. NF-kappaB2/p52 enhances androgen-independent growth of human LNCaP cells via protection from apoptotic cell death and cell cycle arrest induced by androgen-deprivation. Prostate 68, 1725–1733.

Nakamura, H., Wang, Y., Kurita, T., Adomat, H., Cunha, G.R., 2011. Genistein increases epidermal growth factor receptor signaling and promotes tumor progression in advanced human prostate cancer. PLoS One 6, e20034.

Oh, S.J., Erb, H.H., Hobisch, A., Santer, F.R., Culig, Z., 2012. Sorafenib decreases proliferation and induces apoptosis of prostate cancer cells by inhibition of the androgen receptor and Akt signaling pathways. Endocr. Relat. Cancer 19, 305–319.

Oh, W.K., Kantoff, P.W., 1998. Management of hormone refractory prostate cancer: current standards and future prospects. J. Urol. 160, 1220–1229.

Pelton, K., Freeman, M.R., Solomon, K.R., 2012. Cholesterol and prostate cancer. Curr. Opin. Pharmacol. 12, 751–759.

Pienta, K.J., 2001. Preclinical mechanisms of action of docetaxel and docetaxel combinations in prostate cancer. Semin. Oncol. 28, 3–7.

Pommier, A.J., Alves, G., Viennois, E., Bernard, S., Communal, Y., Sion, B., Marceau, G., Damon, C., Mouzat, K., Caira, F., Baron, S., Lobaccaro, J.M., 2010. Liver X receptor activation downregulates AKT survival signaling in lipid rafts and induces apoptosis of prostate cancer cells. Oncogene 29, 2712–2723.

Sarker, D., Reid, A.H., Yap, T.A., de Bono, J.S., 2009. Targeting the PI3K/AKT pathway for the treatment of prostate cancer. Clin. Cancer Res. 15, 4799–4805.

Savli, H., Szendröi, A., Romics, I., Nagy, B., 2008. Gene network and canonical pathway analysis in prostate cancer: a microarray study. Exp. Mol. Med. 40, 176–185.

Sharpless, N.E., Depinho, R.A., 2006. The mighty mouse: genetically engineered mouse models in cancer drug development. Nat. Rev. Drug Discov. 5, 741–754.

Shinka, T., Onodera, D., Tanaka, T., Shoji, N., Miyazaki, T., Moriuchi, T., Fukumoto, T., 2011. Serotonin synthesis and metabolism-related molecules in a human prostate cancer cell line. Oncol. Lett. 2, 211–215.

Siegel, R., Naishadham, D., Jemal, A., 2012. Cancer statistics, 2012. CA Cancer J. Clin. 62, 10–29.

Sobel, R.E., Sadar, M.D., 2005. Cell lines used in prostate cancer research: a compendium of old and new lines – part 1. J. Urol. 173, 342–359.

Solskov, L., Magnusson, N.E., Kristiansen, S.B., Jessen, N., Nielsen, T.T., Schmitz, O., Bøtker, H.E., Lund, S., 2012. Microarray expression analysis in delayed cardioprotection: the effect of exercise, AICAR, or metformin and the possible role of AMP-activated protein kinase (AMPK). Mol. Cell Biochem. 360, 353–362.

Stein, C.A., 1999. Mechanisms of action of taxanes in prostate cancer. Semin. Oncol. 26, 3–7.

Tabaczar, S., Koceva-Chyła, A., Matczak, K., Gwoździński, K., 2010. [Molecular mechanisms of antitumor activity of taxanes. I. Interaction of docetaxel with microtubules]. Postepy. Hig. Med. Dosw. (Online) 64, 568–581.

Tannock, I.F., de Wit, R., Berry, W.R., Horti, J., Pluzanska, A., Chi, K.N., Oudard, S., Théodore, C., James, N.D., Turesson, I., Rosenthal, M.A., Eisenberger, M.A., Investigators, T., 2004. Docetaxel plus prednisone or mitoxantrone plus prednisone for advanced prostate cancer. N. Engl. J. Med. 351, 1502–1512.

Tian, T., Nan, K.J., Guo, H., Wang, W.J., Ruan, Z.P., Wang, S.H., Liang, X., Lu, C.X., 2010. PTEN inhibits the migration and invasion of HepG2 cells by coordinately decreasing MMP expression via the PI3K/Akt pathway. Oncol. Rep. 23, 1593–1600.

Tokunaga, E., Kataoka, A., Kimura, Y., Oki, E., Mashino, K., Nishida, K., Koga, T., Morita, M., Kakeji, Y., Baba, H., Ohno, S., Maehara, Y., 2006. The association between Akt activation and resistance to hormone therapy in metastatic breast cancer. Eur. J. Cancer 42, 629–635.

Tung, W.L., Wang, Y., Gout, P.W., Liu, D.M., Gleave, M., 2011. Use of irinotecan for treatment of small cell carcinoma of the prostate. Prostate 71, 675–681.

Vander Heiden, M.G., Cantley, L.C., Thompson, C.B., 2009. Understanding the Warburg effect: the metabolic requirements of cell proliferation. Science 324, 1029–1033.

Wang, Y., Revelo, M.P., Sudilovsky, D., Cao, M., Chen, W.G., Goetz, L., Xue, H., Sadar, M., Shappell, S.B., Cunha, G.R., Hayward, S.W., 2005a. Development and characterization of efficient xenograft models for benign and malignant human prostate tissue. Prostate 64, 149–159.

Wang, Y., Xue, H., Cutz, J.C., Bayani, J., Mawji, N.R., Chen, W.G., Goetz, L.J., Hayward, S.W., Sadar, M.D., Gilks, C.B., Gout, P.W., Squire, J.A., Cunha, G.R., Wang, Y.Z., 2005b. An orthotopic metastatic prostate cancer model in SCID mice via grafting of a transplantable human prostate tumor line. Lab Invest. 85, 1392–1404.

Watahiki, A., Wang, Y., Morris, J., Dennis, K., O'Dwyer, H.M., Gleave, M., Gout, P.W., 2011. MicroRNAs associated with metastatic prostate cancer. PLoS One 6, e24950.

Wu, C., Wyatt, A.W., McPherson, A., Lin, D., McConeghy, B.J., Mo, F., Shukin, R., Lapuk, A.V., Jones, S.J., Zhao, Y., Marra, M.A., Gleave, M.E., Volik, S.V., Wang, Y., Sahinalp, S.C.,

Collins, C.C., 2012. Poly-gene fusion transcripts and chromothripsis in prostate cancer. Genes Chromosom. Cancer 51, 1144—1153.

Wu, X., Senechal, K., Neshat, M.S., Whang, Y.E., Sawyers, C.L., 1998. The PTEN/MMAC1 tumor suppressor phosphatase functions as a negative regulator of the phosphoinositide 3-kinase/Akt pathway. Proc. Natl. Acad. Sci. U S A 95, 15587—15591.

Xin, L., Teitell, M.A., Lawson, D.A., Kwon, A., Mellinghoff, I.K., Witte, O.N., 2006. Progression of prostate cancer by synergy of AKT with genotropic and nongenotropic actions of the androgen receptor. Proc. Natl. Acad. Sci. U S A 103, 7789—7794.